

SHAPING THE GLOBULAR CLUSTER MASS FUNCTION BY STELLAR-DYNAMICAL EVAPORATION

DEAN E. McLAUGHLIN¹

University of Leicester, Department of Physics and Astronomy, University Road, Leicester, UK LE1 7RH

AND

S. MICHAEL FALL

Space Telescope Science Institute, 3700 San Martin Drive, Baltimore, MD 21218

submitted to The Astrophysical Journal

ABSTRACT

We show that the globular cluster mass function (GCMF) in the Milky Way depends on cluster half-mass density, ρ_h , in the sense that the mass M_{TO} at which the GCMF turns over increases with ρ_h while the width of the distribution decreases. We argue that this behavior is expected if a peak in the GCMF is the result of slow depletion, predominantly through cluster evaporation driven by internal two-body relaxation, of a mass function that originally rose as a power law towards low masses—a process previously shown by Fall & Zhang to explain the shape of the current GCMF below M_{TO} . We fit the full GCMF as a function of ρ_h with models in which the average past mass-loss rates of clusters are estimated from their current densities according to $-dM/dt = \mu_{\text{ev}} \propto \rho_h^{1/2}$. The normalization of this μ_{ev} implies total lifetimes that may be slightly on the short side but are well within the range of standard values for the evaporation of tidally limited clusters. We also combine our models with distributions of ρ_h versus Galactocentric radius (r_{gc}) and cluster concentration, both taken directly from observations, to show consistency with known aspects of the GCMF as a function of these other variables. In particular, we recover in this way the well-known insensitivity of M_{TO} to r_{gc} . This feature does not derive from a literal “universality” of the GCMF peak mass, but from a significant variation of M_{TO} with ρ_h , which is fundamentally as expected to result from relaxation-driven cluster disruption, plus a scattered relation between ρ_h and r_{gc} . Our analysis does not depend on any theoretical assumptions or empirical information about the anisotropy profile or any other aspect of the velocity distribution of the Galactic GC system.

Subject headings: galaxies: star clusters—globular clusters: general

1. INTRODUCTION

An important point of reference in attempting to understand the connection between old globular clusters (GCs) and the young massive clusters in local starbursts and galaxy mergers, is the distribution of the cluster masses. When expressed as the number of globulars per unit logarithmic mass, $dN/d \log M$, the GC mass function (GCMF) is characterized by a peak, or turnover, at a mass $M_{\text{TO}} \approx 1\text{--}2 \times 10^5 M_{\odot}$ that is empirically very similar in most galaxies. By contrast, the mass functions of young clusters show no such feature but instead rise monotonically towards low masses, from $M \sim 10^6 M_{\odot}$ down to $M \sim 10^4 M_{\odot}$ in the best-studied cases, in a way that is well described by a power law, $dN/d \log M \propto M^{1-\beta}$ with $\beta \simeq 2$ (e.g., Zhang & Fall 1999).

Nonetheless, at high $M > M_{\text{TO}}$, old GCMFs do closely resemble the mass functions of young clusters, and of molecular clouds in the Milky Way and other galaxies (Harris & Pudritz 1994; Elmegreen & Efremov 1997); and it is well known that a number of dynamical processes cause star clusters to lose mass, and can lead to their complete destruction, as they orbit for a Hubble time in the tidal fields of their parent galaxies (e.g., Fall & Rees 1977; Caputo & Castellani 1984; Aguilar, Hut, & Ostriker 1988; Chernoff & Weinberg 1990; Gnedin & Ostriker 1997; Murali & Weinberg 1997). It is therefore natural to ask whether the peaks in GCMFs can be explained by the depletion over many Gyr of globulars with $M \lesssim 10^5 M_{\odot}$,

from mass distributions that were originally similar to those of young clusters below M_{TO} as well as above. This possibility is the main focus of this paper.

Our chief purpose is to establish and interpret an aspect of the Galactic GCMF, which appears fundamental but has gone unnoticed to date: $dN/d \log M$ has a strong and systematic dependence on GC half-mass density, $\rho_h \equiv 3M/8\pi r_h^3$ (r_h being the cluster half-mass radius), in the sense that the turnover mass M_{TO} increases and the width of the full distribution decreases with increasing ρ_h . As observed facts, these must be explained by any theory of the GCMF. We argue here that they are an expected signature of slow dynamical evolution from a mass function that initially increased steadily towards $M < M_{\text{TO}}$, if the long-term mass loss from surviving GCs has been dominated by stellar escape due to internal, two-body relaxation (which we refer to from now on as either relaxation-driven evaporation, or simply evaporation).

Fall & Zhang (2001; hereafter FZ01) explain in detail why cluster evaporation dominates the long-term evolution of the low-mass shape of observable GCMFs. Briefly, stellar evolution removes (through supernovae and winds) the same *fraction* of mass from all clusters of a given age, and so cannot change the shape of $dN/d \log M$ (unless special initial conditions are invoked; cf. Vesperini & Zepf 2003). Meanwhile, for GCs like those that have survived for a Hubble time in the Milky Way, the integrated mass loss from gravitational shocks during disk crossings and bulge passages is generally much less than that due to evaporation (see also Gnedin, Lee, & Ostriker 1999; Prieto & Gnedin 2006).²

¹ Current address: School of Physical and Geographical Sciences, Lennard Jones Laboratories, Keele University, Keele, Staffordshire, UK ST5 5BG
Electronic address: dem@astro.keele.ac.uk
Electronic address: fall@stsci.edu

² It is possible that there existed a past population of GCs with low den-

As we discuss further in §2 below, the evaporation of tidally limited clusters proceeds at a rate, $\mu_{\text{ev}} \equiv -dM/dt$, which is nearly constant in time and primarily determined by an appropriate measure of cluster density. FZ01 show that a constant mass-loss rate leads to a power-law scaling $dN/d \log M \propto M^{1-\beta}$ with $\beta \rightarrow 0$ (corresponding to a flat distribution of clusters per unit *linear* mass) at sufficiently low $M < \mu_{\text{ev}} t$ in the evolved mass function of coeval GCs that began with *any* nontrivial initial $dN/d \log M_0$.³ To accommodate this when $dN/d \log M_0$ originally increased towards low masses as a power law, a time-dependent peak must develop in the GCMF at a mass of order $M_{\text{TO}}(t) \sim \mu_{\text{ev}} t$ (FZ01). But then, since μ_{ev} depends fundamentally on cluster density, so too must M_{TO} .

A $\beta \simeq 0$ power-law scaling well below the turnover mass has been confirmed directly in the GCMFs of the Milky Way (FZ01) and the giant elliptical M87 (Waters et al. 2006), while Jordán et al. (2007) show it to be consistent with $dN/d \log M$ data from 89 Virgo Cluster galaxies, and it is apparent in deep observations of some other GCMFs (e.g., in the Sombrero galaxy, M104; Spitler et al. 2006). As regards the peak itself, old GCs are observed (e.g., Jordán et al. 2005) to have rather similar densities on average—and, therefore, similar typical μ_{ev} —in galaxies with widely different total luminosities and Hubble types. (Inasmuch as cluster densities are set by tides, this is probably related to the mild variation of mean *galaxy* density with total luminosity; see the discussion in Jordán et al. 2007, or FZ01.) Thus, an evaporation-dominated evolutionary origin for M_{TO} appears to be consistent with the well-known fact that it generally differs very little between galaxies (e.g., Harris 2001; Jordán et al. 2006).

If this picture is basically correct, then it implies that, even though M_{TO} may appear nearly universal when considering the global mass functions of entire GC systems, in fact the GCMFs of clusters with similar ages but different densities should have different turnovers. In §2, we show—working for definiteness and relatively easy observability with the half-mass density, ρ_h —that this is the case for globulars in the Milky Way. We fit the observed $dN/d \log M$ for GCs in bins of different ρ_h with models assuming that (1) the initial distribution increased as a $\beta = 2$ power law at low masses and (2) the past mass-loss rates of individual clusters can be estimated to first order from their current half-mass densities by the rule $\mu_{\text{ev}} \propto \rho_h^{1/2}$, with a constant of proportionality constrained by the observed, average peak mass of the full GCMF for all Galactic globulars. In §3 we discuss the validity of this prescription for μ_{ev} , which is certainly approximate but captures the main physical dependence of relaxation-driven mass loss. In addition, our normalization of it implies cluster lifetimes that are within a factor of ≈ 2 (on the low side) of typical values in theories and simulations of two-body relaxation in tidally limited GCs.

We also show in §2 that, when our density-dependent model GCMFs are combined with the directly observed distribution of cluster ρ_h versus Galactocentric radius (r_{gc}) they fit the much weaker variation of $dN/d \log M$ and M_{TO} as functions of r_{gc} , which is well known in the Milky Way and other large galaxies (see Harris 2001; Harris, Harris, & McLaughlin

1998; Barmby, Huchra, & Brodie 2001; Vesperini et al. 2003; Jordán et al. 2007). Similarly, convolving the main models with an observed dependence of ρ_h on cluster concentration suffices to account for previously noted differences between the mass functions of low- and high-concentration GCs (Smith & Burkert 2002). The most fundamental feature of the GCMF therefore appears to be its dependence on cluster density, which can be understood at least qualitatively (and even quantitatively, at the roughly factor-of-two level to which our simple models are realistic) in terms of evaporation-dominated cluster disruption.

There is a widespread perception that if the GCMF evolved slowly from a rising power law at low masses, then a weak or null variation of M_{TO} with r_{gc} can be achieved only in GC systems with strongly radially anisotropic velocity distributions, which are not observed (see especially Vesperini et al. 2003). This apparent inconsistency has been cited to bolster some recent attempts to identify a mechanism by which a “universal” peak at $M_{\text{TO}} \sim 10^5 M_{\odot}$ might have been imprinted on the GCMF at the time of cluster formation, or very shortly afterwards, and little affected by the subsequent destruction of lower-mass GCs (e.g., Vesperini & Zepf 2003; Parmentier & Gilmore 2007). However, given the real successes of an evaporation-dominated evolutionary scenario for the origin of M_{TO} , as summarized above and added to below, it would be premature to reject the idea in favor of *requiring* a near-formation origin, solely on the basis of difficulties with GC kinematics. (And, in any event, formation-oriented models must now be reconsidered in light of the *non-universality* of M_{TO} as a function of cluster density.)

We are not concerned in this paper with velocity anisotropy in GC systems, because we only predict an evaporation-evolved $dN/d \log M$ as a function of cluster density (and age) and take the observed distribution of ρ_h versus r_{gc} in the Milky Way as a given, to show consistency with the current (non-)dependence of M_{TO} on r_{gc} . Most other models (FZ01; Vesperini et al. 2003; and references therein) predict dynamically evolved GCMFs directly in terms of r_{gc} , and in doing so are forced also to derive theoretical dependences of ρ_h on r_{gc} . It is only at this stage that GC orbital distributions enter the problem, and then only in conjunction with several other assumptions and simplifications. As we discuss further in §3 below, the unacceptably radially biased GC velocity ellipsoids that appear in such models could well be artifacts of one or more of these other assumptions, rather than of the main hypothesis about evaporation-dominated GCMF evolution.

2. THE GALACTIC GCMF AS A FUNCTION OF CLUSTER DENSITY

In this section we define and model the dependence of the Galactic GCMF on cluster density. First, we describe the dependence that is expected to arise from evaporation-dominated evolution.

Two-body relaxation in a tidally limited GC leads to a fairly steady rate of mass loss, $\mu_{\text{ev}} \equiv -dM/dt \simeq \text{constant}$. Thus, the total cluster mass decreases approximately linearly over time, as $M(t) \simeq M_0 - \mu_{\text{ev}} t$. This behavior is exact in some classic models of GC evolution (e.g., Hénon 1961) and is found to hold well—at least away from the endpoints of the evolution, i.e., usually for $0.9 \gtrsim M(t)/M_0 \gtrsim 0.1$ —in simulations employing many different numerical methods and allowing for a variety of internal cluster properties (see Chernoff & Weinberg 1990; Vesperini & Heggie 1997; Gnedin, Lee, & Ostriker 1999; Baumgardt 2001; Giersz 2001; Baumgardt &

ties or concentrations, or perhaps on extreme orbits, which were destroyed in less than a Hubble time by shocks or stellar evolution. Our discussion does not cover any such clusters.

³ Throughout this paper, we use “initial” to mean at a relatively early time in the development of long-lived clusters, after they have dispersed any remnants of their natal gas clouds, survived the bulk of stellar-evolution mass loss, and come into virial equilibrium in a local tidal field.

Makino 2003; Trenti, Hoggie, & Hut 2007). When gravitational shocks are subdominant to relaxation-driven evaporation, as they generally appear to be for extant GCs, they work to boost the mass-loss rate μ_{ev} slightly without altering the basic linearity of M versus time (e.g., Gnedin, Lee, & Ostriker 1999; see also Figure 1 of FZ01). A time-dependent mass scale of $\Delta \equiv \mu_{\text{ev}} t$ is then associated naturally with any system of coeval GCs with a given mass-loss rate: all clusters with initial $M_0 \leq \Delta$ are disrupted by time t , and replaced with the remnants of objects that began with $M_0 > \Delta$. As we also mentioned in §1, if the initial GCMF increased towards low masses as a power law, then Δ is closely related to a peak in the evolved distribution, which eventually decreases towards very low $M(t) < \Delta$ as $dN/d \log M \propto M^{1-\beta}$ with $\beta = 0$ (FZ01).

In “standard” theory (see Spitzer 1987), the lifetime of a cluster against evaporation is a multiple of its two-body relaxation time, t_{rlx} , at an appropriate, internal (Lagrange) radius r . To first order, ignoring any slight internal velocity-dispersion gradients and a weak mass dependence in the Coulomb logarithm, $t_{\text{rlx}} \sim (Mr^3)^{1/2}$; see, e.g., Section 8.3 of Binney & Tremaine (1987). The instantaneous mass-loss rate is therefore $\mu_{\text{ev}} \equiv -dM/dt \propto M/t_{\text{rlx}} \sim \rho_r^{1/2}$, where $\rho_r \propto M/r^3$ is the average cluster density inside r . A GCMF evolving from an initial $\beta > 1$ power law at low masses should then develop a peak at a mass that depends on cluster density and age, through the parameter $\Delta \sim \rho_r^{1/2} t$. It remains to identify a reference radius such that $\mu_{\text{ev}} \sim \rho_r^{1/2}$ and $\mu_{\text{ev}} \simeq \text{constant}$ in time are mutually consistent.

In a steady tidal field, the mean density ρ_t inside a cluster’s tidal radius is constant by definition, and thus $\mu_{\text{ev}} \propto \rho_t^{1/2}$ is naturally implied. This result is routinely used to set the GC mass-loss rates in models for the dynamical evolution of the GCMF (e.g., Vesperini 1997, 1998, 2000, 2001; Vesperini et al. 2003; Baumgardt 1998; FZ01)—although such studies normally express μ_{ev} immediately in terms of orbital pericenters, r_p , most often by assuming $\rho_t \propto r_p^{-2}$ as for GCs in galaxies whose total mass distributions follow a singular isothermal sphere. This bypasses any explicit examination of the GCMF as a function of cluster density, which is our main goal, but it is done in part because tidal radii are the most poorly constrained of all structural parameters for GCs in the Milky Way (and they are exceedingly difficult, if not impossible to measure in distant galaxies). We deal with this here by focusing on the GCMF as a function of cluster density ρ_h inside the empirically better determined half-mass radius, asking how simple models in which $\mu_{\text{ev}} \propto \rho_h^{1/2}$ fare against the data.

Taking $\mu_{\text{ev}} \propto \rho_h^{1/2}$ in place of $\mu_{\text{ev}} \propto \rho_t^{1/2}$, which we do to construct evaporation-evolved model GCMFs in §2.2, is strictly valid only if the ratio ρ_t/ρ_h is the same for all clusters and fixed in time. This is the case in Hénon’s (1961) model of GC evolution, and in this limit (which is that adopted by FZ01 in their models for the Galactic GCMF) our analysis is rigorously justified. However, real clusters are not homologous (ρ_t/ρ_h differs between clusters) and they do not evolve self-similarly (ρ_h may vary in time even if ρ_t does not). The key assumption in our models is that μ_{ev} is independent of time for any GC, which is well-founded in any case. By using current ρ_h values to estimate μ_{ev} , we do not assume that the half-mass densities are also constant, but we implicitly use a single number for all GCs to represent a variable $(\rho_t/\rho_h)^{1/2}$. Equivalently, we ignore a dependence on central concentration in the ratio of total cluster evaporation time to half-mass

relaxation time (Gnedin & Ostriker 1997). As we discuss further in §3, this is a reasonable first-order approximation because $(\rho_t/\rho_h)^{1/2}$ varies much less among Galactic globulars than ρ_t and ρ_h do separately.

In §3 we also discuss some recent results (Baumgardt 2001; Baumgardt & Makino 2003), which indicate that the timescale for relaxation-driven evaporation depends on a slightly less-than-linear power of t_{rlx} . We note that this ultimately suggests that μ_{ev} may increase as a modest power of cluster *column* density, rather than the usual volume density. We have confirmed that making the appropriate changes throughout the rest of this section to reflect this possibility does not qualitatively change our conclusions.

2.1. Data

Figure 1 shows the distribution of mass against half-mass density and against Galactocentric radius for 146 Milky Way GCs in the catalogue of Harris (1996),⁴ as well as the distribution of ρ_h versus r_{gc} linking the two mass plots. The Harris catalogue actually records the absolute V magnitudes of the GCs; masses follow from applying the individual population-synthesis model mass-to-light ratios Υ_V computed (for an assumed age of 13 Gyr) by McLaughlin & van der Marel (2005), after first multiplying every one by 0.8 to give a median⁵ $\hat{\Upsilon}_V \simeq 1.5 M_{\odot} L_{\odot}^{-1}$ in keeping with direct dynamical estimates (McLaughlin 2000; McLaughlin & van der Marel 2005; Barmby et al. 2007).

Harris (1996) gives the projected half-light radius R_h for 141 of the clusters with a mass estimated in this way, and for these we obtain the three-dimensional half-mass radius from the general rule $r_h = (4/3)R_h$ (Spitzer 1987), which assumes no internal mass segregation. The remaining five objects have mass estimates but no size measurements. To each of these five in turn, we assign an r_h equal to the median value for those of the first 141 GCs having masses within a factor two of the one with unknown r_h . In all cases, the half-mass density is $\rho_h \equiv 3M/8\pi r_h^3$.

The leftmost panel in Figure 1 shows immediately that the cluster mass distribution has a strong dependence on half-mass density: the median \hat{M} increases with ρ_h while the scatter in $\log M$ —that is, the width of the GCMF—decreases. The first of these points is related to the fact that r_h correlates poorly with M (e.g., Djorgovski & Meylan 1994; McLaughlin 2000). The second point, that the dispersion of $dN/d \log M$ decreases with increasing ρ_h , is behind the finding (Kavalaars & Hanes 1997; Gnedin 1997) that the GCMF is broader at very large Galactocentric radii. We return to this in §2.2.

The dashed line in the plot of M versus ρ_h traces the proportionality $M \propto \rho_h^{1/2}$, or $Mr_h^3 = \text{constant}$. Insofar as the half-mass two-body relaxation time scales as $t_{\text{th}} \propto (Mr_h^3)^{1/2}$, and to the extent that $\mu_{\text{ev}} \propto M/t_{\text{th}} \propto \rho_h^{1/2}$ adequately approximates the average rate of relaxation-driven mass loss, this line is one of equal total evaporation time. The fact that such a locus nicely bounds the lower envelope of the observed cluster distribution is by itself a strong hint that relaxation-driven cluster disruption has significantly modified the GCMF at low masses. (Recall also that $Mr_h^3 = \text{constant}$ defines one side of the GC “survival triangle” when the M – ρ_h plot is recast as r_h versus M ; see Fall & Rees 1977, Okazaki & Tosa 1995, Ostriker & Gnedin 1997, and Gnedin & Ostriker 1997).

⁴ Feb. 2003 version; see <http://physwww.mcmaster.ca/~harris/mwgc.dat>.

⁵ Throughout this paper, we use \hat{x} to denote the median of any quantity x .

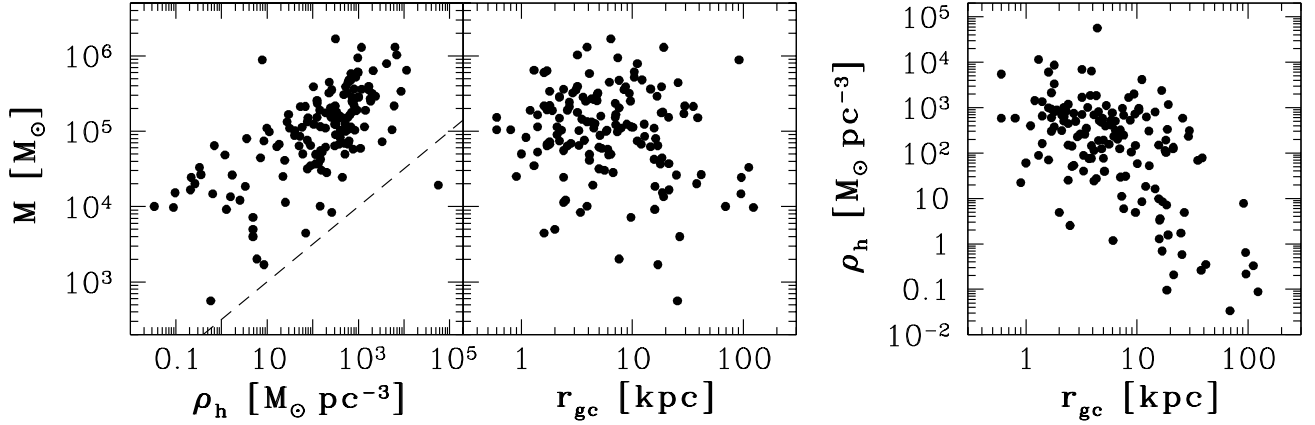


FIG. 1.— *Left*: Mass versus three-dimensional half-mass density, $\rho_h \equiv 3M/8\pi r_h^3$, and versus Galactocentric radius, r_{gc} , for 146 Milky Way GCs in the catalogue of Harris (1996). The dashed line in the first panel is $M \propto \sqrt{\rho_h}$, a locus of approximately constant lifetime against evaporation. *Right*: Half-mass density versus r_{gc} for the same clusters.

The middle panel of Figure 1 shows the well-known result that any measure of “typical” GC mass depends weakly if at all on Galactocentric radius, at least until large $r_{gc} \gtrsim 30$ –40 kpc, where number statistics are poor. The right-hand panel of the figure shows why this is true even though the GCMF does depend significantly on cluster density: While there is a correlation between half-mass density and Galactocentric position, the scatter about it is such that convolving the observed M versus ρ_h with the observed ρ_h versus r_{gc} results in an almost null dependence of M on r_{gc} .

We now divide the GC sample in Figure 1 roughly into thirds, in two different ways: first on the basis of half-mass density, and second by Galactocentric radius. These ρ_h and r_{gc} bins are defined in Table 1, which also gives a few summary statistics for the globulars in each subsample. In each of them we count the clusters in about 10 equal-width bins of $\log M$ first as a function of ρ_h and then as a function of r_{gc} . These GCMFs are shown by the points in Figure 2, with errorbars indicating standard Poisson uncertainties. The curves in the figure trace model GCMFs, which we describe in §2.2. For the moment, it is important to note that the dashed curve is the same in every panel, apart from minor differences in normalization, and is proportional to the average GCMF of all 146 Galactic GCs. (In the middle-left panel of Figure 2, which pertains to clusters distributed tightly around the median ρ_h of the entire GC system, the dashed curve is coincident with the solid curve running through the data.)

Although it is not necessarily obvious from the scatter plots in Figure 1, the left-hand panels of Figure 2 show that the GCMF is peaked for clusters at any density, and that the mass of the peak increases systematically with ρ_h (see also the last column of Table 1, but note that the turnover masses there refer to the *model* GCMFs that we develop below). The statistical significance of this is very high, and qualitatively it is the behavior expected if M_{TO} owes its existence to cluster disruption at rates that increase with ρ_h .

The right-hand panels of Figure 2 confirm once again that the peak of the GCMF is a very weak function of Galactocentric position. In fact, the observed distributions in the two r_{gc} bins inside $\simeq 10$ kpc are statistically indistinguishable in their entirety, and the main difference at larger $r_{gc} \gtrsim 10$ kpc is a slightly higher proportion of low-mass clusters rather than an obvious change in M_{TO} . All of this is consistent with the

primary GCMF dependence being that on ρ_h , since Figure 1 shows that the GC density distribution is quite insensitive to Galactocentric position for $r_{gc} \lesssim 10$ –20 kpc but has a substantial low-density tail (with a broader associated GCMF, as seen in the upper-left panel of Figure 2) at larger radii.

2.2. Simple Models

We now attempt to assess more quantitatively whether these results are consistent with evaporation-dominated evolution of the GCMF from an initial distribution like that observed for young clusters in the local universe. We model the time-evolution of the distribution of M versus ρ_h in Figure 1 but do not attempt the same for the distribution of ρ_h over r_{gc} —the details of which come from a complicated interplay between the tidal field of the Galaxy, the present and past orbital parameters of clusters, and the structural nonhomology of GCs. When comparing our models to the current GCMF as a function of r_{gc} , we simply take ρ_h versus r_{gc} exactly as observed, to effect a change of variable.

Our main assumptions are that the initial GCMF was independent of cluster density, and that any globulars surviving to the present day have been losing mass for the past Hubble time at roughly constant rates. We use the clusters’ *current* half-mass densities to estimate $\mu_{ev} \propto \rho_h^{1/2}$. As we discussed earlier, a nearly time-independent μ_{ev} is indicated robustly by varied numerical simulations of two-body relaxation in tidally limited GCs. We give a more detailed, a posteriori justification in §3 for using ρ_h , which need not be constant in time, to estimate μ_{ev} .

Consider first a group of coeval GCs with an initial mass function $dN/d \log M_0$ and a single, time-independent mass-loss rate μ_{ev} . The mass of every cluster decreases linearly as $M(t) = M_0 - \mu_{ev}t$, and at any later time each has lost the same total amount $\Delta \equiv M_0 - M(t) = \mu_{ev}t$. FZ01 show rigorously that in this case, the evolved and initial GCMFs are related by

$$\frac{dN}{d \log M} = \frac{M}{M_0} \times \frac{dN}{d \log M_0} = \frac{M}{M + \Delta} \frac{dN}{d \log (M + \Delta)}. \quad (1)$$

This is the formal basis for the claim that the mass function scales generically as $dN/d \log M \propto M^{\beta+1}$ (a $\beta = 0$ power law) at low enough $M(t) < \Delta$ —that is, for the surviving remnants of clusters with $M_0 \approx \Delta$ —just so long as the initial distribution was not a delta function.

TABLE 1
MILKY WAY GC PROPERTIES IN BINS OF DENSITY AND GALACTOCENTRIC RADIUS

Bin	\mathcal{N}	$\hat{\rho}_h^a$ [$M_\odot \text{ pc}^{-3}$]	\hat{r}_{gc}^a [kpc]	M_{\min} [M_\odot]	M_{\max} [M_\odot]	\hat{M}^a [M_\odot]	M_{TO}^b [M_\odot]
ρ_h bins							
$0.034 \leq \rho_h \leq 76.5 M_\odot \text{ pc}^{-3}$	48	8.48	12.9	5.63×10^2	8.84×10^5	4.12×10^4	3.98×10^4
$78.8 \leq \rho_h \leq 526 M_\odot \text{ pc}^{-3}$	49	232	5.6	8.37×10^3	1.67×10^6	1.22×10^5	1.58×10^5
$579 \leq \rho_h \leq 5.65 \times 10^4 M_\odot \text{ pc}^{-3}$	49	973	3.2	1.93×10^4	1.30×10^6	2.82×10^5	2.88×10^5
r_{gc} bins							
$0.6 \leq r_{gc} \leq 3.2 \text{ kpc}$	47	597	1.9	4.47×10^3	1.02×10^6	1.15×10^5	2.14×10^5
$3.3 \leq r_{gc} \leq 9.4 \text{ kpc}$	50	261	5.2	2.02×10^3	1.67×10^6	1.27×10^5	1.66×10^5
$9.6 \leq r_{gc} \leq 123 \text{ kpc}$	49	18.4	18.3	5.63×10^2	1.30×10^6	7.42×10^4	8.71×10^4

^aThe notation \hat{x} represents the median of quantity x .

^b M_{TO} is the peak mass of the *model* GCMFs traced by the solid curves in each panel of Figure 2, which are given by equation (3) of the text with $\beta=2$, $M_c = 10^6 M_\odot$, and individual Δ given by the observed ρ_h of each cluster through equation (4).

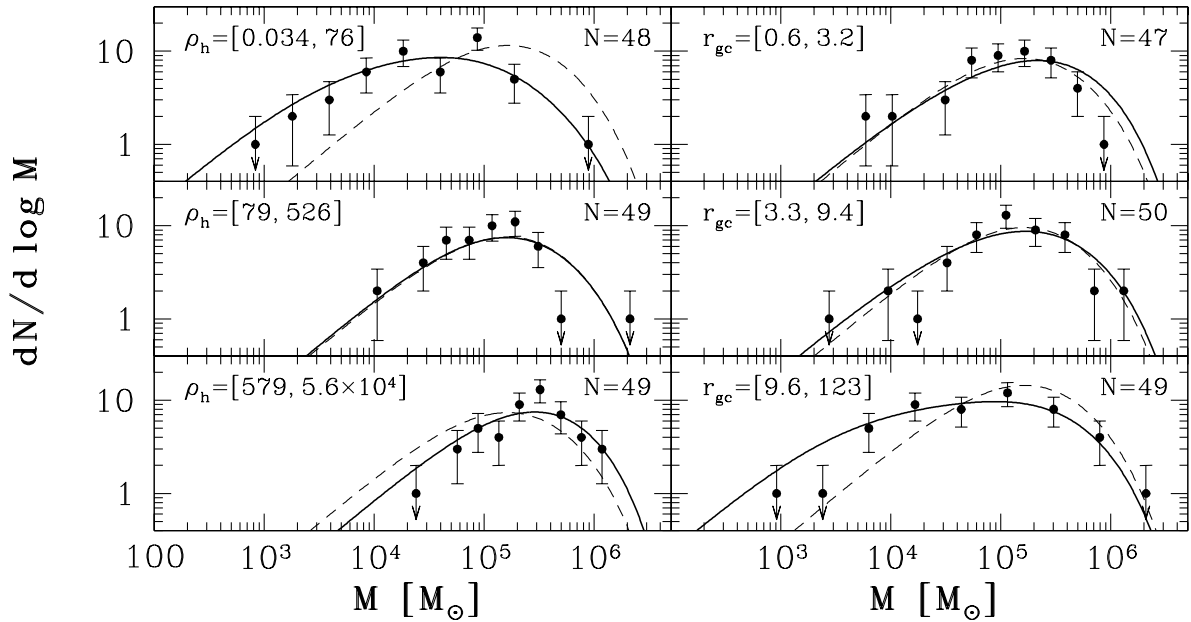


FIG. 2.— GCMF as a function of half-mass density, $\rho_h \equiv 3M/8\pi r_h^3$ (left panels), and as a function of Galactocentric radius, r_{gc} (right panels), for 146 Milky Way GCs in the catalogue of Harris (1996). The dashed curve in all cases is an evolved Schechter function for the entire GC system (Jordán et al. 2007): equation (3) with $\beta = 2$, $M_c = 10^6 M_\odot$, and $\Delta \equiv 2.3 \times 10^5 M_\odot$ for all clusters (from eq. [4]) and a median $\hat{\rho}_h = 246 M_\odot \text{ pc}^{-3}$, giving a peak at $M_{\text{TO}} = 1.6 \times 10^5 M_\odot$. Solid curves are the GCMFs predicted by equation (3) with $\beta = 2$ and $M_c = 10^6 M_\odot$ but individual Δ given by the observed ρ_h of each cluster (eq. [4]).

We follow FZ01 (see also Jordán et al. 2007) in adopting a Schechter (1976) function for the initial GCMF:

$$dN/d \log M_0 \propto M_0^{1-\beta} \exp(-M_0/M_c). \quad (2)$$

With $\beta \simeq 2$, this distribution describes the power-law mass functions of young massive clusters in systems like the Antennae galaxies (e.g., Zhang & Fall 1999). An exponential cut-off at $M_c \sim 10^6 M_\odot$ is generally consistent with such data, even if not always demanded by them; here we require it mainly to match the curvature observed at high masses in old GCMFs (e.g., Jordán et al. 2007; Burkert & Smith 2000).

Combining equations (1) and (2) gives the probability density that a single GC with known evaporation rate and age has an instantaneous mass M . The time-dependent GCMF of a system of \mathcal{N} GCs with a range of μ_{ev} (or ages, or both) is

then just the sum of all such individual probability densities:

$$\frac{dN}{d \log M} = \sum_{i=1}^{\mathcal{N}} \frac{A_i M}{[M + \Delta_i]^\beta} \exp\left[-\frac{M + \Delta_i}{M_c}\right], \quad (3)$$

where the total mass losses $\Delta_i = (\mu_{\text{ev}} t)_i$ may differ from cluster to cluster (t_i being the age of a single GC) but both β and M_c are constants, independent of ρ_h in particular.⁶ Given each Δ_i , the normalizations A_i in equation (3) are defined so that the integral over all masses of each term in the summation is unity.

⁶ Note that M_c appears to take on different values in the GCMFs of other galaxies, varying systematically with the total luminosity L_{gal} (Jordán et al. 2007). The reasons for this are unclear, as is the origin of this mass scale in the first place.

Jordán et al. (2007) have introduced a specialization of equation (3) in which all clusters have the same Δ . They refer to this as an evolved Schechter function and describe its properties in detail for the case $\beta = 2$. We note only that, at very young cluster ages or for slow mass-loss rates, such that $\Delta \ll M_c$ and only the low-mass, power-law part of the initial GCMF is significantly eroded, any one evolved Schechter function has a peak at $M_{\text{TO}} \simeq \Delta/(\beta - 1)$. As Δ increases relative to M_c , the turnover at first increases proportionately and the width of the distribution decreases (since the high-mass end at $M \gtrsim M_{\text{TO}}$ is largely unchanged). For extreme $\Delta \gg M_c$, however, the peak is bounded above by $M_{\text{TO}} \rightarrow M_c$ and the width approaches a lower limit.⁷ Any peak in the full equation (3) for a system of GCs with individual Δ values is an average of \mathcal{N} different turnovers and must be calculated numerically.

In their modeling of the Milky Way GCMF, Fall & Zhang (2001) effectively compute distributions of the type (3)—based on the same initial conditions and dynamical evolution—with individual Δ set by hypothetical orbital parameters of clusters in a spherical and static logarithmic Galaxy potential (used both to fix ρ_h via tidal-limitation arguments, and to determine additional mass loss due to gravitational shocks). Jordán et al. (2007) fit GCMF data in the Milky Way and scores of Virgo Cluster galaxies with their version of equation (3) in which all GCs have the same Δ . They thus estimate the net dynamical mass loss from *typical* clusters in these systems. Here, we construct models for the Milky Way GCMF using Δ values given directly by the observed half-mass densities of individual GCs.

We adopt $\beta = 2$ for the initial low-mass power-law index in equation (2), which carries over into equation (3) for the evolved $dN/d \log M$. Jordán et al. (2007) have fitted the full Galactic GCMF with an evolved Schechter function assuming $\beta = 2$ and a single $\Delta \equiv \hat{\Delta}$ for all surviving globulars. They find $M_c \simeq 10^6 M_\odot$ and $\hat{\Delta} = 2.3 \times 10^5 M_\odot$. We use this value of M_c directly in equation (3) and we associate $\hat{\Delta}$ with the net mass loss from clusters at the median half-mass density of the entire GC system, which is $\hat{\rho}_h = 246 M_\odot \text{pc}^{-3}$ from the data in Figure 1. Since we are assuming that $\Delta \propto \mu_{\text{ev}} \propto \rho_h^{1/2}$ (for coeval GCs), we therefore stipulate

$$\Delta = 1.45 \times 10^4 M_\odot (\rho_h / M_\odot \text{pc}^{-3})^{1/2} \quad (4)$$

for globulars with arbitrary ρ_h . Assuming a typical GC age of 13 Gyr, this corresponds to estimating the average relaxation-driven mass-loss rate of clusters in the past as

$$\mu_{\text{ev}} \simeq 1.1 \times 10^3 M_\odot \text{Gyr}^{-1} (\rho_h / M_\odot \text{pc}^{-3})^{1/2}. \quad (5)$$

In §3 we discuss the net cluster lifetimes implied by this.

The dashed curve shown in every panel of Figure 2 is the evolved Schechter function fit to the entire GCMF by Jordán et al. (2007). It has a peak at the standard value of $M_{\text{TO}} \simeq 1.6 \times 10^5 M_\odot$ (magnitude $M_V \simeq -7.4$ for a typical V -band mass-to-light ratio of 1.5 in solar units) and gives a very good description of the observed $dN/d \log M$ in the middle density bin, $79 \lesssim \rho_h \lesssim 530 M_\odot \text{pc}^{-3}$, and of those in the two inner radius bins, $r_{\text{gc}} \leq 9.4$ kpc. This is expected, since the

median half-mass density in each of these cluster subsamples is very close to the system-wide median $\hat{\rho}_h = 246 M_\odot \text{pc}^{-3}$ (see Table 1). Even in the outermost r_{gc} bin, a Kolmogorov-Smirnov (KS) test only marginally rejects the dashed-line model (at the $\simeq 95\%$ level), because this subsample still includes many GCs at or near the global median $\hat{\rho}_h$ (see Figure 1). By contrast, the average GCMF is strongly rejected as a model for the lowest- and highest-density GCs on the left-hand side of Figure 2: the KS probabilities that these data are drawn from the dashed distribution are $< 10^{-4}$ in both cases. This is also expected, since by construction these bins only contain clusters, with densities well away from the median of the full GC system, for which the net mass lost to evaporation should be significantly different from the typical $\hat{\Delta} = \Delta(\hat{\rho}_h)$.

The solid curves in Figure 2, which are different in every panel, are the full superpositions of evolved Schechter functions in equation (3), with distinct Δ values given by equation (4) using the observed ρ_h of each cluster in the corresponding subsample. They provide excellent matches to the observed $dN/d \log M$ in every ρ_h and r_{gc} bin; χ^2 per degree of freedom is < 1.3 in all cases. This is the main result of this paper.

The last column of Table 1 gives the mass M_{TO} at which each of the solid *model* GCMFs in Figure 2 peaks. We note that these turnovers increase roughly as $M_{\text{TO}} \sim \hat{\rho}_h^{0.3-0.4}$ for our specific choices of binning in ρ_h and r_{gc} , somewhat shallower than the $\rho_h^{1/2}$ scaling of the cluster mass-loss rate, which defines the models. This is partly because of the averaging over many individual turnovers implied by the summation of many evolved Schechter functions in each GC bin, and partly because—as we discussed above, just after equation (3)—an individual M_{TO} cannot increase indefinitely in proportion to $\Delta \propto \rho_h^{1/2}$, but has a strict upper limit of $M_{\text{TO}} \leq M_c$.

Our models are naturally consistent with the fact that the width of the GCMF is smaller for clusters with higher half-mass density. This is obvious in the left-hand panels of Figure 2, and in the discussion immediately after equation (3) we described how it follows from the increase of M_{TO} with $\Delta \propto \rho_h^{1/2}$ for a single evolved Schechter function. In addition, the superposition of many GCMFs with separate, density-dependent turnovers and widths results in wider $dN/d \log M$ for cluster subsamples covering larger ranges of ρ_h . This accounts in particular for the breadth of the mass function at $r_{\text{gc}} \geq 9.4$ kpc. The globulars at these radii span $0.034 \leq \rho_h \leq 4.1 \times 10^3 M_\odot \text{pc}^{-3}$, corresponding to individual evolved Schechter functions with turnovers at $2.7 \times 10^3 \lesssim M_{\text{TO}} \lesssim 4.0 \times 10^5 M_\odot$. The composite GCMF in the lower-right panel of Figure 2 therefore shows an extremely flat peak, such that an overall M_{TO} cannot be established precisely from the data alone. The full width at half-maximum is correspondingly larger than in the inner Galaxy, where the ρ_h distribution is much narrower. This explains the findings of Kavelaars & Hanes (1997), who first pointed out that the GCMF of the outermost third of the Milky Way cluster system has a turnover that is statistically consistent with the full-Galaxy average, but a larger dispersion (see also Gnedin 1997).

Finally, if the GCMF evolved dynamically from initial conditions similar to those we have adopted, then the data and models in the left-hand panels of Figure 2 argue against the notion that gravitational shocks, rather than relaxation-driven evaporation, might have mainly driven the evolution of the present GC population. This is because, while evaporation-dominated cluster disruption involves mass-loss rates that in-

⁷ The increase of M_{TO} and the decrease of the full width of $dN/d \log M$ for increasing Δ eventually saturate when the mass loss per GC is so high that it affects clusters in the exponential part of the initial Schechter-function GCMF. This is because $dN/d \log M \propto M^{+1} \exp(-M/M_c)$ is a self-similar solution to the evolution equation (1).

crease as a positive power of GC density, the (negative) mass-loss rate due to shocks alone is inversely proportional to ρ_h : $\mu_{\text{sh}} \propto M/\rho_h$, with a constant of proportionality that depends on details of the GC orbit (i.e., the frequency of disk crossings or bulge passages). Thus, with the GC system split into distinct ρ_h bins as in Figure 2, shock-dominated evolution would be expected to result in the GCMF for the highest-density globulars being *less* evolved, and closer in form to the initial $dN/d \log M_0$, than that for the lowest-density clusters—opposite to what is observed.

2.3. Other Cluster Properties

If the current shape of the GCMF is fundamentally the result of long-term cluster disruption according to a mass-loss “law” like $\mu_{\text{ev}} \propto \rho_h^{1/2}$, then in principle it should be possible to describe $dN/d \log M$ as a function of any other cluster property, by using the observed distribution of densities versus that other property to transform our models in §2.2—as we did when matching them to the GCMF in different bins of r_{gc} . Distinct mass functions can of course be constructed for any number of cluster subsystems, and some are bound to differ from others. Here we explore one example, in which differences in $dN/d \log M$ for two groups of GCs can be traced to different ρ_h distributions.

Smith & Burkert (2002) note that the mass function of Galactic globulars with King (1966) model concentrations $c < 0.99$ has a less massive peak than that for $c \geq 0.99$. [Here $c \equiv \log(r_t/r_0)$, where r_t is a fitted tidal radius and r_0 a core scale.] They further show that a power-law fit to the low- c GCMF just below its peak returns $dN/d \log M \propto M^{+0.5}$, shallower than the M^{+1} expected generically for a mass-loss rate that is constant in time (and which Smith & Burkert confirm for the GCMF at $c \geq 0.99$). They discuss various options to explain these results, including a suggestion that, if the mass functions of both low- and high-concentration clusters evolved slowly from the same, young-cluster like initial distribution, then the mass-loss law for low- c GCs may have differed from that for high- c clusters. However, they give no physical argument for such a difference, and we can show now that none is required.

The upper panel of Figure 3 plots concentration against half-mass density for the same 146 GCs from Figure 1; the filled circles distinguish 24 clusters with $c < 0.99$. There is a correlation of sorts between c and ρ_h , which ultimately either derives from or causes the better-known correlation between c and M (e.g., Djorgovski & Meylan 1994; McLaughlin 2000). The important point here is that the ρ_h distribution is offset to lower values and has a higher dispersion at $c < 0.99$. Following the discussion in §2.2, we therefore *expect* the low-concentration GCMF to have a less massive M_{TO} , a flatter shape around the peak, and a larger full width than the high-concentration $dN/d \log M$.

The lower panel of Figure 3 shows the GCMFs for $c < 0.99$ (filled circles) and $c \geq 0.99$ (open circles). The curves are again given by equation (3) with $\beta = 2$, $M_c = 10^6 M_\odot$, and individual Δ related to the observed ρ_h through equation (4). These models peak at $M_{\text{TO}} \simeq 4.3 \times 10^4 M_\odot$ for the $c < 0.99$ cluster subsample but at $M_{\text{TO}} \simeq 1.8 \times 10^5 M_\odot$ for $c \geq 0.99$, entirely as a result of the different ρ_h involved. The larger width of $dN/d \log M$ and its shallower slope at any $M \lesssim 10^5 M_\odot$ for the low-concentration GCs are also clear, in both the data and the model curves. It is further evident that there are no low- c Galactic globulars with $M \gtrsim 2 \times 10^5 M_\odot$, i.e., above the

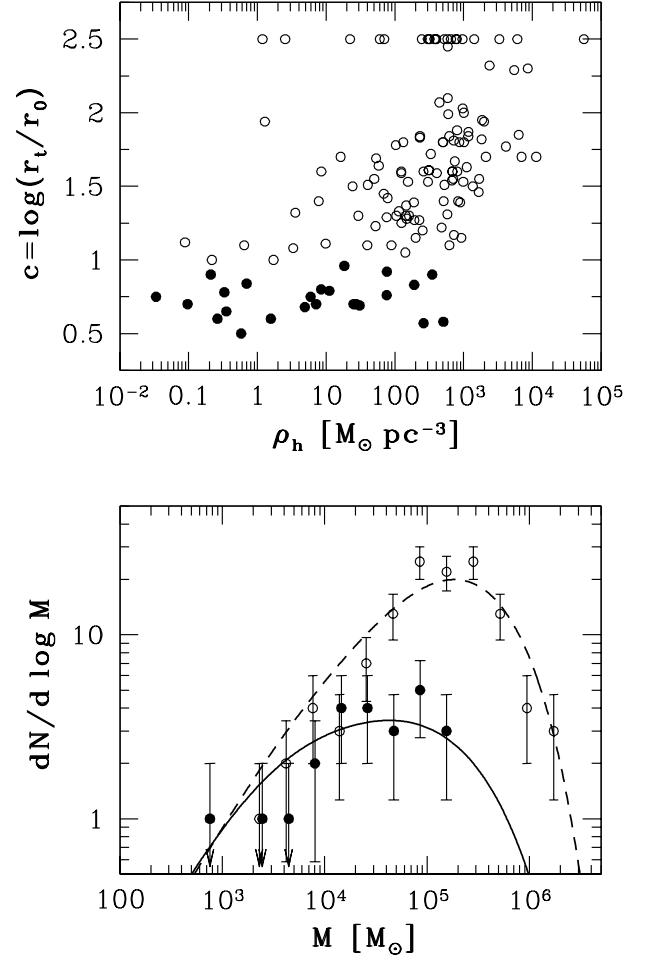


FIG. 3.— *Top*: Concentration parameter as a function of half-mass density for 146 Galactic GCs. The line of points at $c \equiv 2.5$ comes from the practice of assigning this value to core-collapsed clusters in the Harris (1996) catalogue and its sources. *Bottom*: GCMF data and models (eqs. [3] and [4]) for 24 clusters with $c < 0.99$ (filled circles and solid curve) and 122 clusters with $c \geq 0.99$ (open circles and dashed curve).

nominal turnover of the full GCMF (as Smith & Burkert 2002 noted). But this is not surprising, given that there are so few low-concentration clusters in total and they are expected to be dominated by low-mass objects because of their generally low densities. Thus, the solid curve in Figure 3 predicts perhaps $\simeq 3$ high-mass clusters with $c < 0.99$, where none are found.

The apparent variation of the Milky Way GCMF with central concentration is therefore consistent with the same density-based model for evaporation-dominated dynamical evolution, which we compared to $dN/d \log M$ as a function of ρ_h and r_{gc} in §2.2. To show this, we have taken the distribution of ρ_h versus c exactly as observed in the two concentration bins indicated in Figure 3, to transform our models into the curves shown in the lower graph there—just as we also took the ρ_h distribution as a function of r_{gc} directly from the data to match our models to the observed distributions in the right-hand panels of Figure 2. Of course, this is not the same as *explaining* the distribution of ρ_h versus r_{gc} or c . While doing so would be of interest in its own right, it is beyond the scope of our work here.

3. DISCUSSION

In this section, we first show that the mass-loss rate in equation (5) above implies net cluster lifetimes that com-

pare rather favorably with those normally associated with relaxation-driven evaporation. Then we discuss why it is reasonable to approximate $\mu_{\text{ev}} \propto \rho_h^{1/2}$ in the first place. Finally, we touch on the issue of possible conflict, in some other models for evaporation-dominated GCMF evolution, between the near-constancy of M_{TO} as a function of r_{gc} and the observed kinematics of GC systems.

3.1. Cluster Lifetimes

Defining a relaxation-driven disruption time $t_{\text{dis}} = M/\mu_{\text{ev}}$ for a GC of mass M , and working in units of the relaxation time at the half-mass radius, t_{rh} (eq. [8-72] of Binney & Tremaine 1987), equation (5) leads to

$$t_{\text{dis}}/t_{\text{rh}} = M/(\mu_{\text{ev}} t_{\text{rh}}) \simeq 0.9 \ln \Lambda \approx 10, \quad (6)$$

in which an average stellar mass of $0.7 M_{\odot}$ is assumed for all clusters and the Coulomb logarithm is $\ln \Lambda = 8.7\text{--}13.3$ for $M = 10^4\text{--}10^6 M_{\odot}$. This result depends on the median V-band mass-to-light ratio adopted for the Galactic GCs, as $t_{\text{dis}}/t_{\text{rh}} \propto \hat{\Upsilon}_V^{-1/2}$. This is because a linear scaling $\mu_{\text{ev}} \propto \Upsilon_V$ is required to fit the peak mass of a GCMF derived from cluster luminosities (the direct observables), whereas M/t_{rh} is proportional to $\rho_h^{1/2} \propto \Upsilon_V^{1/2} (L/r_h^3)^{1/2}$. Recall that the median mass-to-light ratio in this paper is $\hat{\Upsilon}_V \simeq 1.5 M_{\odot} L_{\odot}^{-1}$ (§2.1).

The coefficients in our expressions for Δ and $\mu_{\text{ev}} = \Delta/(13 \text{ Gyr})$ as functions of ρ_h (eqs. [4] and [5]) are specific to the choice $\beta = 2$ for the power-law exponent at low masses in the initial GCMF (eq. [2]). As we mentioned just after equation (3), the turnover mass of an evolved Schechter function is $M_{\text{TO}} \simeq \Delta/(\beta-1)$ in the limit of low $\Delta \propto \rho_h^{1/2}$, and $M_{\text{TO}} \rightarrow M_c$ for very high Δ . In this sense, Δ is most strongly constrained by the low-density clusters. All other things being equal, their observed GCMF can be reproduced with $\beta \neq 2$ if Δ and μ_{ev} are multiplied by $(\beta-1)$ at fixed ρ_h . Equation (6) then becomes $t_{\text{dis}}/t_{\text{rh}} \simeq 10/(\beta-1)$. Observations of young massive clusters (e.g., Zhang & Fall 1999) constrain β to be near 2; but if it were slightly shallower, then the relative lifetimes we infer would increase accordingly.

In the model of Hénon (1961) for self-similar GC evaporation (fixed ratio ρ_t/ρ_h of mean densities inside the tidal and half-mass radii) in a steady tidal field (constant ρ_t), a cluster loses 4.5% of its remaining mass every half-mass relaxation time. The time to complete disruption is therefore $t_{\text{dis}}/t_{\text{rh}} = 1/0.045 \simeq 22$. For non-homologous clusters in a steady tidal field, $t_{\text{dis}}/t_{\text{rh}}$ is a function of central concentration and can differ from the Hénon value by factors of about two. From one-dimensional Fokker-Planck calculations, Gnedin & Ostriker (1997) find $t_{\text{dis}}/t_{\text{rh}} \simeq 10\text{--}40$ for King (1966) model clusters with the range of c values found in real GCs. Estimates from other methods are generally similar (e.g., Vesperini & Heggie 1997; Takahashi & Portegies Zwart 2000), although noticeably shorter lifetimes are certainly possible (Baumgardt 2001; Baumgardt & Makino 2003), and there is always some imprecision due to differences in the detailed physics and numerics in different studies (see the discussions of Takahashi & Portegies Zwart 1998, 2000; Baumgardt 2001; Joshi, Nave, & Rasio 2001; Giersz 2001).

Thus, while the cluster lifetimes implied by our fitting of evaporation-evolved model GCMFs to the Milky Way may appear slightly shorter than usual, they are clearly within the range of t_{dis} values calculated from first principles in theories of two-body relaxation in tidally limited GCs. Ultimately, it

is encouraging to find consistency to within a factor of two between two estimates of a quantity by such vastly different methods. This is especially so, given that part of the difference between our $t_{\text{dis}}/t_{\text{rh}} \approx 10$, and the more familiar $t_{\text{dis}}/t_{\text{rh}} \sim 20$, is surely due to disk and bulge shocks having modestly enhanced the average mass-loss rates of the real clusters to which our models are normalized (although, again, shocks do not appear to have dominated the evolution of extant GCs in general and are not expected to affect the basic time-independence of a net μ_{ev} ; see Gnedin, Lee, & Ostriker 1999, FZ01, and Prieto & Gnedin 2006). It is also worth emphasizing that the results of Hénon (1961) and Gnedin & Ostriker (1997) specifically apply to single-mass GCs on circular orbits in spherical galaxy potentials. Clusters with a realistic spectrum of stellar masses may evaporate somewhat faster (e.g., Johnstone 1993; Lee & Goodman 1995), and GCs on circular orbits are longer-lived than those on eccentric orbits with the same apocenter in the same potential (Baumgardt & Makino 2003). Indeed, according to Baumgardt & Makino, $t_{\text{dis}}/t_{\text{rh}}$ may be reduced by a full factor of two for an orbital eccentricity $e \simeq 0.5$, which is typical for a tracer population with an isotropic velocity distribution in a logarithmic potential (van den Bosch et al. 1999).

3.2. Approximating $\mu_{\text{ev}} \propto \rho_h^{1/2}$

Because $t_{\text{rh}} \propto M/\rho_h^{1/2}$ and we have used GC half-mass densities to estimate $\mu_{\text{ev}} \propto \rho_h^{1/2}$, our result for $t_{\text{dis}}/t_{\text{rh}}$ in equation (6) is independent of other cluster properties. As mentioned above, however, the Fokker-Planck calculations of Gnedin & Ostriker (1997) in particular show that $t_{\text{dis}}/t_{\text{rh}}$ is in fact a function of central concentration. We have computed $(\rho_t/\rho_h)^{1/2} = (r_h/r_t)^{3/2}$ versus concentration for King-model clusters, finding a curve that is almost identical in shape to the dependence of the inverse lifetime $t_{\text{rh}}/t_{\text{dis}}$ on c in Figure 6 of Gnedin & Ostriker. Thus, their average evaporation rates can be written as $\mu_{\text{ev}} \propto \rho_t^{1/2}$ with a constant of proportionality that is nearly independent of c . This is in keeping with our discussion at the beginning of §2, and it implies that our equations (4) and (5) give an acceptable first-order approximation to evaporation-dominated cluster mass loss, only to the extent that it is valid to treat $(\rho_t/\rho_h)^{1/2}$ as roughly the same for all GCs.

By fitting for the coefficient in $\Delta = \mu_{\text{ev}} t$ to define our models, we have effectively ensured that it already includes an appropriate, average value of $(\rho_t/\rho_h)^{1/2}$ for Galactic globulars. The full range of all possible values for $(\rho_t/\rho_h)^{1/2}$ in King-model clusters with $c \gtrsim 0.7$ (central potential $W_0 \gtrsim 3$) is only a factor of $\lesssim 4$ between minimum and maximum (which is reflected in the similar range of $t_{\text{dis}}/t_{\text{rh},0}$ in Gnedin & Ostriker 1997), and so assuming a single, intermediate value for all GCs should only ever be in error by a factor of about 2 at worst. Therefore, only small relative inaccuracies are expected to result from setting $\mu_{\text{ev}} \propto \rho_h^{1/2}$ for GCs with a spread of four to five orders of magnitude in measured density. We have confirmed this directly, by repeating the analysis of §2 in full but using ρ_t (derived, rather uncertainly in most cases, from the data in Harris 1996) in place of ρ_h throughout. All of our main results persist: The basic character of all panels in Figure 1 is the same, and the peak mass of the GCMF increases systematically and significantly with ρ_t . Moreover, the observed $dN/d \log M$ in bins of ρ_t , r_{gc} , and c , analogous to those in Figures 2 and 3, are fit as well as before by the sums of evolved $\beta = 2$ Schechter functions, once ρ_t is substituted

for ρ_h in equations (4) and (5) and the numerical coefficients there are multiplied by a constant factor of ≈ 13 , the median value of $(\rho_h/\rho_t)^{1/2}$ for all Galactic GCs.

Perhaps of more concern, Baumgardt (2001) and Baumgardt & Makino (2003) have concluded from N -body simulations that the total evaporation times of tidally limited clusters are not simply multiples of an internal two-body relaxation time, t_{rlx} , but scale as $t_{\text{dis}} \propto t_{\text{rlx}}^x t_{\text{cr}}^{1-x}$, where $t_{\text{rlx}} \propto (Mr^3)^{1/2}$ as usual; the crossing time $t_{\text{cr}} \propto (M/r^3)^{-1/2}$; and $x \lesssim 1$ in general (Baumgardt 2001 and Baumgardt & Makino 2003 find $x \simeq 0.75$ – 0.8). The reason for this is that, while stars are scattered to near- and above-escape energies in a relaxation time, they do not actually cross the tidal radius and leave the cluster instantaneously once they have achieved such energies (see also Takahashi & Portegies Zwart 1998, 2000; Fukushima & Heggie 2000). The dependence on crossing time when $x < 1$ in Baumgardt’s expression for t_{dis} reflects the finite timescale for the loss of unbound stars from clusters, which is further tied up with details of the stellar orbits and the local tidal field. On the other hand, the arguments and simulations that imply $x < 1$ assume steady or smoothly varying tidal fields; they do not include the effects of regular disk and bulge shocks. In principle, these may speed up the stripping of stars scattered by relaxation into GC halos, effectively bringing x back nearer to 1 and t_{dis} closer to the standard dependence on t_{rlx} only. It is also unlikely that a single scaling with $x < 1$ can hold for systems with arbitrary numbers of stars, N , since for large enough N it would imply an unphysical $t_{\text{dis}} < t_{\text{th}}$ (see Baumgardt 2001 for further discussion). In any case, note that Baumgardt (2001) and Baumgardt & Makino (2003) still find that $\mu_{\text{ev}} = -dM/dt$ is roughly constant in time.

For general x , evaluating the relevant timescales in $t_{\text{dis}} \propto t_{\text{rlx}}^x t_{\text{cr}}^{1-x}$ at the tidal radius r_t yields $t_{\text{dis}} \propto M^{x-1/2} r_t^{3/2}$. This scaling is identical (apart from our neglect of the Coulomb logarithm) to that obtained by combining equations (1) and (7) of Baumgardt & Makino (2003). It corresponds to an average mass-loss rate $\mu_{\text{ev}} = M/t_{\text{dis}} \propto M^{3/2-x} r_t^{-3/2}$, which—to keep our emphasis on cluster densities—can be re-written in terms of the column density $\Sigma_t = M/\pi r_t^2$ and the usual volume density $\rho_t = 3M/4\pi r_t^3$: $\mu_{\text{ev}} \propto \Sigma_t^{3(1-x)} \rho_t^{2(x-3/4)}$. Clearly, the standard $\mu_{\text{ev}} \propto \rho_t^{1/2}$, which we have already discussed, is recovered with $x = 1$; while with $x = 0.75$, as in the analyses of Baumgardt (2001) and Baumgardt & Makino,⁸ we have the equally straightforward $\mu_{\text{ev}} \propto \Sigma_t^{3/4}$.

We have therefore repeated all of our analyses in §2 again, this time with $\rho_h^{1/2}$ replaced everywhere by $\Sigma_t^{3/4}$ estimated from the Harris (1996) catalogue data, and we have again found very similar results: the lower boundary of a plot of cluster $\log M$ against $\log \Sigma_t$ has a slope of about $3/4$, and the scatter in Σ_t as a function of r_{gc} is substantial; the peak of the GCMF increases with increasing Σ_t ; and the full $dN/d \log M$ as a function of Σ_t , r_{gc} , or c is fit well by evolved Schechter functions based on equations (4) and (5) for Δ and μ_{ev} , with $(\rho_h/M_\odot \text{pc}^{-3})^{1/2}$ replaced by $(\Sigma_t/M_\odot \text{pc}^{-2})^{3/4}$ but keeping the same numerical coefficients. It is not obvious why this should

be the case, but it reflects the fact that Galactic GC data are consistent with the extremely simple relation $\rho_h/M_\odot \text{pc}^{-3} \approx (\Sigma_t/M_\odot \text{pc}^{-2})^{1.5}$ (in the mean; there is scatter about this). Ultimately, this because the observed correlation between central concentration and cluster mass (Djorgovski & Meylan 1994; McLaughlin 2000) combines with the intrinsic dependence of r_t/r_h on c in King models to give $(r_t/r_h) \sim M^{1/6}$.

Thus, although our adopted $\mu_{\text{ev}} \propto \rho_h^{1/2}$ is rigorously self-consistent only in restricted circumstances, it turns out to be a reasonable approximation to more sophisticated and general descriptions of evaporation-dominated cluster mass loss.

3.3. M_{TO} versus r_{gc} , and Velocity Anisotropy in GC Systems

In this paper we have directly predicted $dN/d \log M$ as a function only of GC density and age, and relied on the observed distribution of ρ_h versus r_{gc} in order to infer the current dependence of our model GCMFs on Galactocentric radius. Most other models in the literature for evaporation-dominated GCMF evolution, in either the Milky Way or other systems, instead predict the distribution explicitly as a function of r_{gc} at any time. They therefore need, in effect, to derive theoretical density-position relations for clusters in galaxies alongside their main GCMF calculations. This usually begins with the adoption of analytical potentials to describe the parent galaxies of GCs. Taking these to be spherical and static for a Hubble time allows the use of standard tidal-limitation formulae to write the densities of GCs ab initio in terms of the (fixed) pericenters r_p of unique orbits in the adopted potentials. Cluster relaxation times and net mass-loss rates μ_{ev} then follow as functions of r_p as well. Finally, specific initial mass, space, and velocity (or orbital eccentricity) distributions are chosen for entire GC systems, so that at all later times it is known what the dynamically evolved $dN/d \log M$ is for globulars with any single r_p , how many clusters with a given r_p survive, and what the distributions of r_p and all dependent cluster properties are at any instantaneous position r_{gc} .

In this approach, if the GCMF began with a $\beta \simeq 2$ power-law rise towards low masses and its current peak is due entirely to cluster disruption, then a strong dependence of M_{TO} on r_p is expected because the densities of tidally limited GCs decrease with increasing r_p . Thus, models along these lines that assume the orbit distribution of a GC system to be the same at all radii in a galaxy (i.e., that the typical ratio r_{gc}/r_p is independent of position) generally have difficulty in accounting for the extremely weak correlation between M_{TO} and observable r_{gc} in large galaxies (see, e.g., Baumgardt 1998; Vesperini 2001; or the “scale-free” models of FZ01).

FZ01 showed (their “Eddington” models) that, if all other assumptions are unchanged, an outwards-increasing radial velocity anisotropy in the initial GC system can resolve this problem in principle: the eccentricity of a typical cluster orbit then increases with galactocentric distance, such that globulars spread over a larger range of current r_{gc} can have more similar r_p and associated M_{TO} . However, the initial velocity-anisotropy gradient required to fit the Milky Way GCMF data specifically may be stronger than allowed by observations of the current GC-system kinematics (e.g., Dinescu, Girard, & van Altena 1999). Subsequently, Vesperini et al. (2003) have constructed broadly similar models for the GCMF of the Virgo elliptical M87 and concluded that there, too, a variable radial velocity anisotropy is required to match the observed M_{TO} versus r_{gc} ; but the model anisotropy profile in this case is clearly inconsistent with the isotropic velocity distribution

⁸ Baumgardt & Makino (2003) simulate clusters with initial King-model central potentials $W_0 = 5$ and $W_0 = 7$ (concentrations $c \simeq 1.0$ and $c \simeq 1.5$). They suggest that the exponent x and the normalization in $t_{\text{dis}} \propto M^{x-1/2} r_t^{3/2}$ differ slightly for the two different concentrations. However, they have many more results for $W_0 = 5$ than for $W_0 = 7$, and all of the lifetimes recorded in their Table 1 can be recovered to within $\lesssim 20\%$ with a single $x = 0.75$ and a single normalization for t_{dis} .

that is actually observed for the GCs out to large r_{gc} (Romanowsky & Kochanek 2001; Côté et al. 2001).

These results certainly suggest that some element is lacking in standard, r_{gc} -oriented GCMF models constructed as outlined above. But they do not show that the fault must lie with the main hypothesis, that the difference between the mass functions of young clusters and old GCs is due to the effects of slow, relaxation-driven disruption in the latter case. Any conclusions about velocity anisotropy depend on all the other steps taken to connect ρ_h to r_{gc} , and it is entirely possible that reasonable changes to the details of one or more of these ancillary assumptions might make the models compatible with the observed kinematics of GCs in the Milky Way and M87, without abandoning a basic physical picture of the GCMF that is otherwise rather successful.

One potential issue is that prior models have always specified the rate of relaxation-driven evaporation as a function of cluster density (or r_p) a priori, usually normalizing μ_{ev} so that $t_{dis}/t_{rh,0} \simeq 20$ –40 in accordance with standard results from theoretical studies of two-body relaxation. However, following our discussion in §3.1, it would seem worthwhile to investigate the usual GCMF models with μ_{ev} increased at fixed ρ_h or r_p to allow $t_{dis}/t_{rh,0} \approx 10$ in general. It is not clear in detail how such a change would affect the velocity-anisotropy profiles inferred by FZ01 or Vesperini et al. (2003). Qualitatively, however, it should weaken the amount of radial-orbit bias required to fit the observed M_{TO} versus r_{gc} , since a given M_{TO} at a given r_{gc} could then be obtained for less dense clusters with larger r_p , i.e., less eccentric orbits.

More generally, FZ01 have emphasized the importance of the standard starting assumption that GCs orbit in galaxies which are spherical and perfectly static. In reality, large galaxies grow hierarchically, in which case much of the burden for the thorough radial mixing of GC systems, required to weaken or erase any initial gradients in M_{TO} versus r_{gc} , may be transferred from velocity anisotropy to the time-dependent evolution of the galaxies themselves. Violent relaxation, major mergers, and smaller accretion events all work to move clusters between different parts of galaxies and between different progenitors, scrambling and combining numerous pericenter-density- M_{TO} relations of the type expected for static galaxies. Any position dependences in the GC ρ_h distribution and in M_{TO} itself for the final galaxy are therefore bound to be weaker, more scattered, and more difficult to relate accurately to a cluster velocity distribution than in the case of a monolithic, unevolving potential.

In our view, the kinematics of GC systems cannot be used as decisive side constraints on theories for the GCMF until these and any other questions about the full range of ingredients in current models have been fully explored, most likely through sophisticated, cosmological N -body simulations.

4. CONCLUSIONS

We have shown that the mass function $dN/d \log M$ of globular clusters in the Milky Way depends significantly on cluster half-mass density, ρ_h , with the peak or turnover mass M_{TO} increasing and the width of the distribution decreasing as ρ_h increases. This behavior is expected if the GCMF initially rose monotonically towards low masses, as observed for young clusters in local starbursts and merging galaxies, and has attained its current shape via the slow depletion of low-mass clusters over Gyr timescales, primarily through relaxation-

driven evaporation. Our results thus add to previous arguments supporting this interpretation of the GCMF, based on the fact that it scales as $dN/d \log M \propto M^{1-\beta}$ with $\beta \simeq 0$ in the low-mass limit (Fall & Zhang 2001).

The observed GCMF as a function of ρ_h is fit well by simple models in which the initial distribution was a Schechter function, $dN/d \log M_0 \propto M_0^{1-\beta} \exp(-M_0/M_c)$ with $\beta = 2$ and $M_c \simeq 10^6 M_\odot$, and in which clusters have been losing mass for a Hubble time at roughly steady rates that can be estimated from their current half-mass densities as $\mu_{ev} \propto \rho_h^{1/2}$. We have argued that, although this prescription is approximate, it accurately captures the main physical dependence of relaxation-driven evaporation. Using the observed peak mass of the GCMF for the entire Galactic GC system to constrain the normalization of μ_{ev} at a given ρ_h leads to total cluster lifetimes of $t_{dis}/t_{rh} \approx 10$ in units of their half-mass relaxation times—slightly shorter than, but within range of the values typically obtained in theoretical studies of two-body relaxation in tidally limited clusters.

Combining our density-dependent models of dynamically evolved GCMFs with directly observed distributions of cluster ρ_h against central concentration c and Galactocentric radius r_{gc} yields model $dN/d \log M$ as functions of c and of r_{gc} , which again fit observations well. This suggests that the most fundamental physical dependence in the GCMF is that on cluster density.

Our transformed models for $dN/d \log M$ versus r_{gc} in particular are fully consistent with the well-known insensitivity of the GCMF peak mass to Galactocentric position. We have not invoked an unrealistically anisotropic GC velocity distribution to achieve this consistency; indeed, we have made no predictions or assumptions whatsoever about velocity anisotropy. We have emphasized that, when velocity anisotropy enters other long-term dynamical-evolution models for the GCMF, it is only in conjunction with several additional, interrelated assumptions made as part of larger efforts to derive theoretical ρ_h - r_{gc} relations for GCs—which we have not attempted to do here. The apparent need in some current models, for a strong bias towards high-eccentricity cluster orbits in order to explain the near-constancy of M_{TO} versus r_{gc} , might well be avoided by changing one or more of their ancillary assumptions rather than by discarding the underlying idea, that the peak and low-mass shape of the GCMF are the result of slow, relaxation-driven cluster disruption.

One advantage to estimating approximate, past mass-loss rates for GCs from their current half-mass densities is that ρ_h can be measured for globulars in many galaxies beyond the Local Group. Thus, the main ideas in this paper can be tested and refined using vastly larger datasets than that available in the Milky Way. For example, Chandar, Fall, & McLaughlin (2007) have recently shown that the peak mass of the GCMF in the Sombbrero galaxy (M104) also increases with ρ_h , in a way that is reasonably well described by the same type of models that we have developed here. It would be of interest to see if the result holds still more generally.

We thank Michele Trenti, Douglas Heggie, Bill Harris, and Rupali Chandar for helpful discussions and comments. SMF acknowledges support from NASA grant AR-09539.1-A, awarded by the Space Telescope Science Institute, which is operated by AURA, Inc., under NASA contract NAS5-26555.

REFERENCES

- Aguilar, L., Hut, P., & Ostriker, J. P. 1988, *ApJ*, 335, 720
- Barmby, P., Huchra, J. P., & Brodie, J. P. 2001, *AJ*, 121, 1482
- Barmby, P., McLaughlin, D. E., Harris, W. E., Harris, G. L. H., & Forbes, D. A. 2007, *AJ*, 133, 2764
- Baumgardt, H. 1998, *A&A*, 330, 480
- Baumgardt, H. 2001, *MNRAS*, 325, 1323
- Baumgardt, H., & Makino, J. 2003, *MNRAS*, 340, 227
- Binney, J., & Tremaine, S. 1987, *Galactic Dynamics* (Princeton: Princeton University Press)
- Burkert, A., & Smith, G. H. 2000, *ApJ*, 542, L95
- Caputo, F., & Castellani, V. 1984, *MNRAS*, 207, 185
- Chandar, R., Fall, S. M., & McLaughlin, D. E. 2007, *ApJ*, in press (arXiv:0709.1440)
- Chernoff, D. F., & Weinberg, M. D. 1990, *ApJ*, 351, 121
- Côté, P., et al. 2001, *ApJ*, 559, 828
- Dinescu, D. I., Girard, T. M., & van Altena, W. F. 1999, *AJ*, 117, 1792
- Djorgovski, S., & Meylan, G. 1994, *AJ*, 108, 1292
- Elmegreen, B. G., & Efremov, Y. N. 1997, *ApJ*, 480, 235
- Fall, S. M., & Rees, M. J. 1977, *MNRAS*, 181, 37P
- Fall, S. M., & Zhang, Q. 2001, *ApJ*, 561, 751 (FZ01)
- Fukushige, T., & Heggie, D. C. 2000, *MNRAS*, 318, 753
- Giersz, M. 2001, *MNRAS*, 324, 218
- Gnedin, O. Y. 1997, *ApJ*, 487, 663
- Gnedin, O. Y., & Ostriker, J. P. 1997, *ApJ*, 474, 223
- Gnedin, O. Y., Lee, H. M., & Ostriker, J. P. 1999, *ApJ*, 522, 935
- Harris, W. E. 1996, *AJ*, 112, 1487
- Harris, W. E. 2001, in *Star Clusters* (28th Saas-Fee Advanced Course) ed. L. Labhardt & B. Binggeli (Berlin: Springer), 223
- Harris, W. E., & Pudritz, R. E. 1994, *ApJ*, 429, 177
- Harris, W. E., Harris, G. L. H., & McLaughlin, D. E. 1998, *AJ*, 115, 1801
- Hénon, M. 1961, *Ann. d'Astrophys.*, 24, 369
- Johnstone, D. 1993, *AJ*, 105, 155
- Joshi, K. J., Nave, C. P., & Rasio, F. A. 2001, *ApJ*, 550, 691
- Jordán, A., et al. 2005, *ApJ*, 634, 1002
- Jordán, A., et al. 2006, *ApJ*, 651, L25
- Jordán, A., et al. 2007, *ApJS*, 171, 101
- Kavelaars, J. J., & Hanes, D. A. 1997, *MNRAS*, 285, L31
- Lee, H. M., & Goodman, J. 1995, *ApJ*, 443, 109
- King, I. R. 1966, *AJ*, 71, 276
- McLaughlin, D. E. 2000, *ApJ*, 539, 618
- McLaughlin, D. E., & van der Marel, R. P. 2005, *ApJS*, 161, 304
- Murali, C., & Weinberg, M. D. 1997, *MNRAS*, 291, 717
- Okazaki, T., & Tosa, M. 1995, *MNRAS*, 274, 48
- Ostriker, J. P., & Gnedin, O. Y. 1997, *ApJ*, 487, 667
- Parmentier, G., & Gilmore, G. 2007, *MNRAS*, 377, 352
- Prieto, J. L., & Gnedin, O. Y. 2006, preprint (astro-ph/0608069)
- Romanowsky, A. J., & Kochanek, C. S. 2001, *ApJ*, 553, 722
- Schechter, P. 1976, *ApJ*, 203, 297
- Smith, G. H., & Burkert, A. 2002, *ApJ*, 578, L51
- Spitzer, L., Larsen, S. S., Strader, J., Brodie, J. P., Forbes, D. A., & Beasley, M. A. 2006, *AJ*, 132, 1593
- Spitzer, L. 1987, *Dynamical Evolution of Globular Clusters* (Princeton: Princeton Univ. Press)
- Takahashi, K., & Portegies Zwart, S. F. 1998, *ApJ*, 503, L49
- Takahashi, K., & Portegies Zwart, S. F. 2000, *ApJ*, 535, 759
- Trenti, M., Heggie, D. C., & Hut, P. 2007, *MNRAS*, 374, 344
- van den Bosch, F. C., Lewis, G. F., Lake, G., & Stadel, J. 1999, *ApJ*, 515, 50
- Vesperini, E. 1997, *MNRAS*, 287, 915
- Vesperini, E. 1998, *MNRAS*, 299, 1019
- Vesperini, E. 2000, *MNRAS*, 318, 841
- Vesperini, E. 2001, *MNRAS*, 322, 247
- Vesperini, E., & Heggie, D. C. 1997, *MNRAS*, 289, 898
- Vesperini, E., & Zepf, S. E. 2003, *ApJ*, 587, L97
- Vesperini, E., Zepf, S. E., Kundu, A., & Ashman, K. M. 2003, *ApJ*, 593, 760
- Waters, C. Z., Zepf, S. E., Lauer, T. R., Baltz, E. A., & Silk, J. 2006, *ApJ*, 650, 885
- Zhang, Q., & Fall, S. M. 1999, *ApJ*, 527, L81